

A Higher Order Synergistic Damage Model for Prediction of Stiffness Changes due to Ply Cracking in Composite Laminates

Chandra Veer Singh^{1,2}

Abstract: A non-linear damage model is developed for the prediction of stiffness degradation in composite laminates due to transverse matrix cracking. The model follows the framework of a recently developed synergistic damage mechanics (SDM) approach which combines the strengths of micro-damage mechanics and continuum damage mechanics (CDM) through the so-called constraint parameters. A common limitation of the current CDM and SDM models has been the tendency to over-predict stiffness changes at high crack densities due to linearity inherent in their stiffness-damage relationships. The present paper extends this SDM approach by including higher order damage terms in the characterization of ply cracking damage inside the material. Following the SDM procedure, predictions are aided by suitable micromechanical computations of crack opening displacements. A nonlinear SDM model is developed and applied for multiple classes of composite laminate layups. Stiffness predictions for damaged laminates using the developed model are compared with the experimental data for cross-ply ($[0_m/90_n]_s$), angle-ply ($[\pm\theta_m/90_n]_s$), off-axis ($[0/\pm\theta_4/0_{1/2}]_s$) and quasi-isotropic ($[0/90/\mp 45]_s$) laminates. A comparison with current linear damage models showcases the usefulness of the proposed nonlinear SDM approach.

Keywords: Composite materials, modeling, transverse cracking, damage mechanics, multiple damage modes.

1 Introduction

Due to their high stiffness to weight ratios, modern composite materials are widely used for structural applications in aerospace, automotive, electronics, energy, and

¹ Department of Materials Science & Engineering, University of Toronto, 184 College St, Suite 140, Toronto, Ontario M5S 3E4, Canada.

² Corresponding author: Tel.: +1 416 946 5211; Fax: +1 416 978 4155.
E-mail: chandraveer.singh@utoronto.ca

sports industries. During service, they are subjected to a combination of mechanical and thermal loadings. Consequently, the material develops damage in form of inter-laminar and intra-laminar cracking, fiber breakage, and debonding. In many cases, intralaminar cracking occurs first, wherein an array of matrix cracks form in the transverse plies. Being unstable in nature, these cracks grow quickly through the lamina width and thickness; at which point they are arrested at the ply interfaces. Upon the application of external loading, the crack surfaces open and slide, thereby reducing the average strain and stress in the damaged layers. This leads to a reduction in the effective thermoelastic properties of the laminate. Understanding the initiation and progression of such ply cracks; and their effect on the overall stiffness properties of the composite laminate has been an important area of research in the past four decades. The developed damage models are either based on micro mechanical solutions to the boundary value problem of laminates with ply cracks, e.g. Hashin (1985); Gudmundson and Ostlund (1992); McCartney (1992); Lundmark and Varna (2005); or they utilize homogenized continuum damage mechanics (CDM) approaches, e.g. Talreja (1985); Allen, Harris and Groves (1987). Only a few of these approaches are applicable to the case of multidirectional laminates which contain developed cracks in multiple orientations, i.e. leading to a multi-mode scenario. A recently published book by Talreja and Singh (2012) provides a comprehensive review of the issues and analysis methods involved in the damage and failure of composite materials.

The CDM methodology has been successfully applied to predict stiffness changes due to intralaminar damage in a variety of composite laminates. However, its applicability for laminates with general layup has been often limited due to requirements for experimental testing in order to determine a number of phenomenological damage constants. Talreja (1996) made a significant advance by proposing that CDM and micromechanics can be combined to enable application of CDM without having to resort to experimental data everytime the laminate layup changes. This approach, termed as synergistic damage mechanics (SDM) uses the concept of a constraint parameter, which is calculated through the computational micromechanics. SDM then incorporates this information into stiffness-damage relations obtained in the CDM framework, along with the material constants determined from experimental/numerical data for a *reference* laminate sequence (usually cross-ply). Initially, the SDM approach was utilized for stiffness predictions in $[\pm\theta/90_s]_s$ laminates [Varna, Joffe and Talreja (2001)] with ply cracking damage in 90° layers. More recently, it has been extended to the case of multidirectional laminates with multi-mode damage scenarios. It has been shown to work well for $[0/\pm\theta_4/0_{1/2}]_s$ and $[0_m/\pm\theta_n/90_r]_s$ laminates [Varna, Joffe, Akshantala and Talreja (1999); Singh and Talreja (2008, 2009)]. The SDM approach is also a participant model in the

ongoing World-Wide Failure Exercise (WWFE III) wherein its predictions [Singh and Talreja (2013)] will be tested against independent experimental investigations. Despite above advancements, a key limitation of both CDM and SDM models is that their predictions show linear variation in the stiffness changes with an increase in ply crack density. This may work well in the early stages of damage development as the experimental results show significant (and almost linear) degradation in stiffness properties. However, the test data over a large variety of composite materials and laminate layups suggest that as the number of ply cracks in a given volume increases, the rate of change in the stiffness properties reduces, leading to almost negligible degradation rate at large crack density levels (> 1.0 crack per unit thickness of the cracked ply). This non-linearity in stiffness changes occurs due to crack shielding effect; when the average spacing between neighboring cracks becomes very small, their stress fields start interacting. Furthermore, it is expected that there will be a limiting minimum stiffness due to contributions from uncracked plies. Hence, linear models of CDM and SDM tend to over-predict stiffness degradation at high crack density.

An effort is made in the present work to extend SDM approaches to include higher order damage terms and to enable prediction of stiffness changes at high crack densities. The free energy expression necessary to derive stiffness relations is expanded to include non-linear damage terms; and the corresponding stiffness-damage relations are derived for multiple laminate layups. Predictions using linear and the proposed non-linear model are compared with the available experimental results for angle ply, off-axis and quasi-isotropic laminates.

2 Nonlinear SDM Approach for Stiffness Degradation

Consider a laminate with a mix of longitudinal and off-axis plies loaded axially, as shown in Fig. 1. On loading, one of the transverse plies will attain the critical stress state necessary for initiation of matrix cracking. A further increase in applied loading causes multiple matrix cracking by the shear-lag process. If the load is increased even more, ply cracks would appear in multiple off-axis plies. These cracks dissipate energy by conducting surface displacements, thereby leading to a decrease in the overall stiffness properties of the composite material. Ply cracks can also lead to more critical damage mechanisms such as delamination, which in turn can cause catastrophic failure of the composite structure. This problem of progressive failure from transverse cracks consists of two subproblems: (1) predicting the evolution of crack density as a function of the applied load; and (2) the evaluation of stiffness changes brought out by ply cracks. For the damage evolution sub-problem, an accurate model based on energetics of ply cracking has been described in our recent papers [Singh and Talreja (2010, 2013)]. The present paper

concerns the second sub-problem.

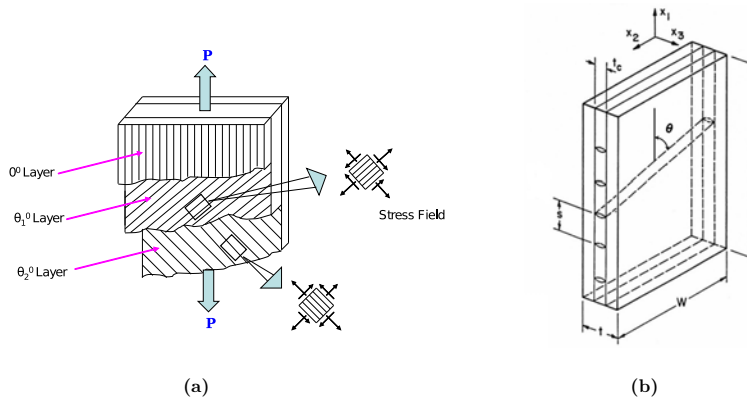


Figure 1: (a) An off-axis laminate loaded in axial tension, and (b) an RVE illustrating off-axis cracking.

Fig. 1(b) shows a *representative volume element* (RVE) illustrating one set of intralaminar cracks in an off-axis ply of a composite laminate. Although for clarity of illustration the cracking is shown only in one lamina, it is understood that in general it exists in multiple plies of the laminate. This damage development consisting of ply cracks in multiple orientations represents a multi-mode damage scenario. For characterizing the effects of this damage on the overall elastic response of the multidirectional laminate, the notions of continuum damage mechanics (CDM) as developed by Talreja (1985) are utilized. The CDM approach characterizes this damage through the homogenization of evolving microstructure involving damage entities over an RVE. The resulting damage field around a point inside the material is then described by a second order damage tensor which defines damage state in an equivalent homogenized continuum. The physical aspects of damage mode tensor definition are described in Talreja (1990, 1994); Singh and Talreja (2013) in detail. However, for the sake of completeness, important concepts are covered here. Inside the RVE, an individual damage entity (a crack or void) can be viewed as bounded by a surface S , on which any point can be associated with two vectors: \mathbf{a} and \mathbf{n} , where \mathbf{a} represents a selected influence of the damage entity; and \mathbf{n} is the unit outward normal to the surface. The effect of damage is then described by the surface integral of dyadic product of the vector components $a_i n_j$, i.e.

$$d_{ij} = \int_S a_i n_j dS \quad (1)$$

The total set of damage entities can be grouped into individual damage modes,

each representing a subset of entities that have the same geometrical characteristics (orientation, shape, etc.). For example, matrix cracks in one ply orientation may constitute one damage mode, while fibre/matrix debonds may constitute another. By homogenizing d_{ij} of a given damage mode α over the RVE, the damage mode tensor is defined as

$$D_{ij}^{(\alpha)} = \sum_{k\alpha=1}^N (d_{ij})_{k\alpha} \quad (2)$$

where N is the number of damage entities of a given mode in the RVE. For the particular case of intralaminar cracking in composite laminates (Fig. 1), the volume of the RVE, V , the surface area of a crack, S , and the influence vector magnitude, a , are specified as

$$V = L.W.t \quad (3)$$

$$S = \frac{W.t_c}{\sin \theta} \quad (4)$$

$$a = \kappa.t_c \quad (5)$$

where t_c is the thickness of the cracked plies, s is the average crack spacing, t is the total laminate thickness, and W and L stand for the width and the length, respectively, of the RVE. Here κ , called the constraint parameter, is an unspecified constant of (assumed) proportionality between a and the crack size t_c (also cracked-ply thickness). Here, $0 \leq \theta \leq \pi/2$, so that S is always positive. Assuming a to be constant over the crack surface S , the damage tensor elements for damage mode α are given by:

$$D_{ij}^{(\alpha)} = \frac{\kappa t_c^2}{st \sin \theta} n_i n_j \quad (6)$$

where $n_i = (\sin \theta, \cos \theta, 0)$ are components of the unit vector normal to the matrix crack plane in the off-axis ply in the global coordinate system $X_i, i=1,2,3$. κ , known as the constraint parameter, represents the constraint effects of surrounding plies on the cracked plies.

The constitutive relations for the damaged laminate can be derived from the specific Helmholtz free energy involving terms in strain and damage elements. In order to include nonlinear effects of damage, we consider damage terms up to the second order. The relation between the specific Helmholtz free energy and the stress tensor is given by:

$$\sigma_{ij} = \rho \frac{\partial \psi \left(\varepsilon_{ij}, D_{ij}^{(\alpha)} \right)}{\partial \varepsilon_{ij}} \quad (7)$$

Consider first the case of thin ply laminates and a single damage mode. Using the Voigt notation, the stress and damage state is characterized by: $\varepsilon_{11} = e_1$, $\varepsilon_{22} = e_2$, $\varepsilon_{12} = e_6$; $D_{11} = D_1$, $D_{22} = D_2$, and $D_{12} = D_6$. Please note that the superscript for damage mode α is dropped to represent the case of single damage mode. The most general polynomial form for Helmholtz free energy (ψ), restricted to second order terms in the strain and damage tensor components, is given by

$$\begin{aligned} \rho\psi = & P_0 + P_1(e_p, D_q) + P_2(D_q) + P_3(D_q^2) \\ & + \{c_1e_1^2 + c_2e_2^2 + c_3e_6^2 + c_4e_1e_2\} + \{c_5D_1 + c_6D_2\}e_1^2 + \{c_7D_1 + c_8D_2\}e_2^2 \\ & + \{c_9D_1 + c_{10}D_2\}e_6^2 + \{c_{11}D_1 + c_{12}D_2\}e_1e_2 + c_{13}D_6e_1e_6 + c_{14}D_6e_2e_6 \\ & + \{c_{15}D_1^2 + c_{16}D_2^2\}e_1^2 + \{c_{17}D_1^2 + c_{18}D_2^2\}e_2^2 + \{c_{19}D_1^2 + c_{20}D_2^2\}e_6^2 \\ & + \{c_{21}D_1^2 + c_{22}D_2^2\}e_1e_2 + c_{23}D_6^2e_1e_6 + c_{24}D_6^2e_2e_6 \end{aligned} \quad (8)$$

where ρ is the mass density, c_i are material constants, P_0 is a constant, P_1 is a linear function of strain and damage tensor components, and P_2, P_3 are the linear and quadratic function of damage tensor components, respectively. Setting the free energy to zero for unstrained and undamaged material, we have, $P_0 = 0$, and assuming the unstrained material of any damaged state to be stress-free, we get $P_1 = 0$. Similar expression for ψ can be written for the case of multiple damage modes. Using Eq. (7) for in-plane response, we obtain the following elastic stiffness tensor of the cracked laminate with multiple damage modes (see the appendix of Singh and Talreja (2009) for details of derivation):

$$C_{pq} = C_{pq}^0 + \sum_{\alpha} C_{pq}^{(\alpha)} \quad (9)$$

where, $p, q = 1, 2, 6$, C_{pq}^0 are the elements of the stiffness coefficient matrix of the pristine laminate and $\sum_{\alpha} C_{pq}^{(\alpha)} = C_{pq} - C_{pq}^0 = \Delta C_{pq}$ represents the stiffness change due to matrix cracking averaged (homogenized) over the RVE. The components of these stiffness tensors for a single mode of damage, including non-linear terms in damage tensor, are derived as:

$$C_{pq}^0 = \begin{bmatrix} 2c_1 & c_4 & 0 \\ c_4 & 2c_2 & 0 \\ 0 & 0 & 2c_3 \end{bmatrix} = \begin{bmatrix} \frac{E_1^0}{1-\nu_{12}^0\nu_{21}^0} & \frac{\nu_{12}^0E_2^0}{1-\nu_{12}^0\nu_{21}^0} & 0 \\ \frac{\nu_{12}^0E_2^0}{1-\nu_{12}^0\nu_{21}^0} & \frac{E_2^0}{1-\nu_{12}^0\nu_{21}^0} & 0 \\ 0 & 0 & G_{12}^0 \end{bmatrix} \quad (10)$$

$$C_{pq}^{(1)} = \begin{bmatrix} 2c_5D_1 + 2c_6D_2 & c_{11}D_1 + c_{12}D_2 & c_{13}D_6 \\ \text{Symm} & 2c_7D_1 + 2c_8D_2 & c_{14}D_6 \\ & & 2c_9D_1 + 2c_{10}D_2 \end{bmatrix} \quad (11)$$

$$C_{pq}^{(2)} = \begin{bmatrix} 2c_{15}D_1^2 + 2c_{16}D_2^2 & c_{21}D_1^2 + c_{22}D_2^2 & c_{23}D_6^2 \\ & 2c_{17}D_1^2 + 2c_{18}D_2^2 & c_{24}D_6^2 \\ Symm & & 2c_{19}D_1^2 + 2c_{20}D_2^2 \end{bmatrix} \quad (12)$$

where $c_k, k = 1, 2, \dots, 24$ denotes the phenomenological constants.

For axial loading, it can be assumed that $D_1 \gg D_2, D_6$. Note here that by doing so, we are neglecting the shear deformation effects and considering only the components which are normal to the crack surface. This works for cracked plies close to $\theta = 90^\circ$. Following the procedure described in Singh and Talreja (2008, 2009, 2013), and including the second order damage components, we obtain

$$C_{pq} = C_{pq}^0 + D[a_i] + D^2[b_i] \quad (13)$$

with

$$[a_i] = \begin{bmatrix} 2a_1 & a_4 & 0 \\ & 2a_2 & 0 \\ Symm & & 2a_3 \end{bmatrix}; \quad [b_i] = \begin{bmatrix} 2b_1 & b_4 & 0 \\ & 2b_2 & 0 \\ Symm & & 2b_3 \end{bmatrix} \quad (14)$$

where a_i and $b_i, i = 1, 2, 3, 4$ represent the damage constants. Note that we have reduced the total number of phenomenological constants to be evaluated from 20 in Eqs. (10)-(12) to 8 in above expressions.

The damage constants are determined from the stiffness degradation results for a *reference* laminate. In most cases, it is chosen as the cross-ply laminate so that the necessary data can be acquired in multiple ways: (i) by using independent experimental data for stiffness changes with respect to crack density, see e.g. Varna, Joffe, Akshantala and Talreja (1999), or (ii) by using an accurate analytical model such as a variational approach [Hashin (1985)], or (iii) by performing a numerical study such as the finite element method (FEM), see e.g. Singh and Talreja (2009). The damage constants are then computed as follows:

$$\Delta C_{pq} = D[a_i] + D^2[b_i] \quad (15)$$

$$\text{At crack density } s = s_1 \text{ or } \rho = \rho_1 : \Delta C_{pq}(\rho_1) = D_1[a_i] + D_1^2[b_i] \quad (16)$$

$$\text{At crack density } s = s_2 \text{ or } \rho = \rho_2 : \Delta C_{pq}(\rho_2) = D_2[a_i] + D_2^2[b_i] \quad (17)$$

Solving above equations, we obtain

$$[a_i] = \frac{1}{D_2 - D_1} \left[\frac{D_1}{D_2} \Delta C_{pq}(\rho_1) - \frac{D_2}{D_1} \Delta C_{pq}(\rho_2) \right] \quad (18)$$

$$[b_i] = \frac{1}{D_2 - D_1} \left[\frac{1}{D_1} \Delta C_{pq}(\rho_2) - \frac{1}{D_2} \Delta C_{pq}(\rho_1) \right] \quad (19)$$

with, $D_1 = D(\rho_1)$; $D_2 = D(\rho_2)$. Once the expressions for stiffness matrix of the damaged laminate are obtained, the corresponding engineering moduli can be derived from the following relationships:

$$E_1 = \frac{C_{11}C_{22} - C_{12}^2}{C_{22}}; \quad E_2 = \frac{C_{11}C_{22} - C_{12}^2}{C_{11}}; \quad \nu_{12} = \frac{C_{12}}{C_{22}}; \quad G_{12} = C_{66} \quad (20)$$

From an energy balance during loading of the cracked laminate, the effect of ply cracks on the overall constitutive response of the damaged composite is provided by the work performed in opening and sliding of crack surfaces. Based on fracture mechanics, the magnitude of the constraint parameter κ (Eq. (6)) can therefore be taken as the crack opening displacement (COD) averaged and normalized with respect to the cracked ply thickness ($= \overline{\Delta u_y}/t_c$). This simple definition of κ is helpful because it can then be determined both experimentally, e.g. Varna, Joffe, Akshantala and Talreja (1999), and numerically (using FEM), e.g. Singh and Talreja (2008, 2009). To allow independent comparison of constitutive response of a given class of laminates with cracks in different orientations, COD is calculated here at a small crack density. However, if one were to predict damage evolution (sub-problem 1), it is noted that the variation of COD with crack density needs to be appropriately accounted for, as covered in Singh and Talreja (2010). κ is also assumed independent of the geometry of the composite body. However, it is noted that in the case of complex interaction between stress concentrators in the component geometry such as a hole, and ply cracks; such an assumption may be rendered invalid. In such cases, κ needs to be recalculated using more detailed stress analysis. Further details of κ determination are covered in the results section. Obviously the constraint parameters and corresponding damage tensor elements will depend on the laminate layup. Hence, we will describe them for different classes of laminate sequences one by one.

2.1 $[\pm\theta_m/90_n]_s$ laminates

For small values of angle ply orientation (θ), the cracks appear in 90° plies only. Thus, only a single damage mode is active. The difference in damage influence for a specific θ can be determined by comparing the amount of opening of cracked surfaces with the opening for the case of the reference cross-ply laminate ($[0_m/90_n]_s$). The influence of crack opening is calculated by the normalized average crack opening displacement (COD), which can be computed numerically (using FEM) see e.g. the papers by Joffe, Krasnikovs and Varna (2001); Singh and Talreja (2008) or experimentally, see e.g. Varna, Akshantala and Talreja (1999); Varna, Joffe, Akshantala and Talreja (1999). The constraint parameter for this case is defined as:

$$\kappa = \frac{\overline{\Delta u_y}}{t_c} \quad (21)$$

where $\overline{\Delta u_y}$ is the average COD, defined as

$$\overline{\Delta u_y} = \frac{1}{t_c} \int_{-t_c/2}^{t_c/2} \Delta u_y(z) dz \tag{22}$$

and Δu_y represents the separation of crack planes in the direction normal to the crack face. To estimate $\overline{\Delta u_y}$ numerically, Δu_y is determined from nodal y-direction (normal to crack longitude) displacements averaged over the entire crack surface. The relative constraint parameter, defined as the ratio of κ for $[\pm\theta_m/90_n]_s$ laminate and κ for the reference crossply ($[0_2/90_4]$) laminate, is determined as

$$\kappa_{rel}(\theta) = \frac{(\overline{\Delta u_y})_{[\pm\theta_m/90_n]_s}}{(\overline{\Delta u_y})_{[0_2/90_4]_s}} \tag{23}$$

2.2 $[0/\pm\theta_4/0_{1/2}]_s$ laminates

Assuming the similarity of damage development, CODs in two symmetric modes ($+\theta$ and $-\theta$ -cracks) can be added together to get $\overline{\Delta(u_y)_{\pm\theta}}$. The validity of this assumption is discussed in the results and discussion section. For the present laminate configuration, the constraint parameter κ_θ normalized by κ_{90} is taken as the average COD of the θ -cracks relative to the average COD of 90° -cracks. Thus,

$$\kappa_{rel}(\theta) = \frac{\kappa_\theta}{\kappa_{90}} = \frac{(\overline{\Delta u_y})_{\pm\theta_4}}{(\overline{\Delta u_y})_{90_8}} \tag{24}$$

It is noted that the COD value in the numerator is the sum of CODs of the $+\theta_4$ and $-\theta_4$ cracks, while the COD in the denominator is of an 8-ply thick 90° -crack. All CODs are calculated at the same imposed displacement on the FE unit cells.

2.3 $[0_m/90_r/\mp\theta_n]_s$ laminates

When ply cracks are present in multiple orientations, there will be a constraint parameter corresponding to each damage mode α , given by

$$\kappa_\alpha = \frac{(\overline{\Delta u_y})_\alpha}{t_{c_\alpha}} \tag{25}$$

For the present laminate configuration, cracks will be present in 3 modes: $+\theta$, $-\theta$ and 90° . The linear SDM model for this case was developed in Singh and Talreja (2009). Following the procedure described in the appendix of the cited reference, an effective damage parameter can be derived as

$$D = \frac{2t_0^2}{t} \left[\frac{1}{s_n^\theta \kappa_\theta|_{\theta=90}} \frac{\kappa_\theta}{\kappa_\theta} \{ 2(2n+r)^2 \kappa_{90_{4n+2r}} - r^2 \kappa_{90} \} + r^2 \frac{\kappa_{90}}{s_{90}^2} \right] \tag{26}$$

where t_0 is the thickness of a single ply, t is the thickness of whole laminate, s_n^θ and s^{90} are the normal crack spacings in $\pm\theta$ and 90° -plies, respectively. The constraint parameters are defined as

$$\kappa_\theta = \frac{(\overline{\Delta u_y})_{\pm\theta_{2n}}}{2nt_0}; \quad \kappa_{90_{4n+2r}} = \frac{(\overline{\Delta u_y})_{90_{4n+2r}}}{(4n+2r)t_0}; \quad \kappa_{90} = \frac{(\overline{\Delta u_y})_{90_{2r}}}{2rt_0} \quad (27)$$

where a subscript denotes a particular damage mode (orientation of cracked plies) and sub-subscript represents the number of cracked plies corresponding to that damage mode.

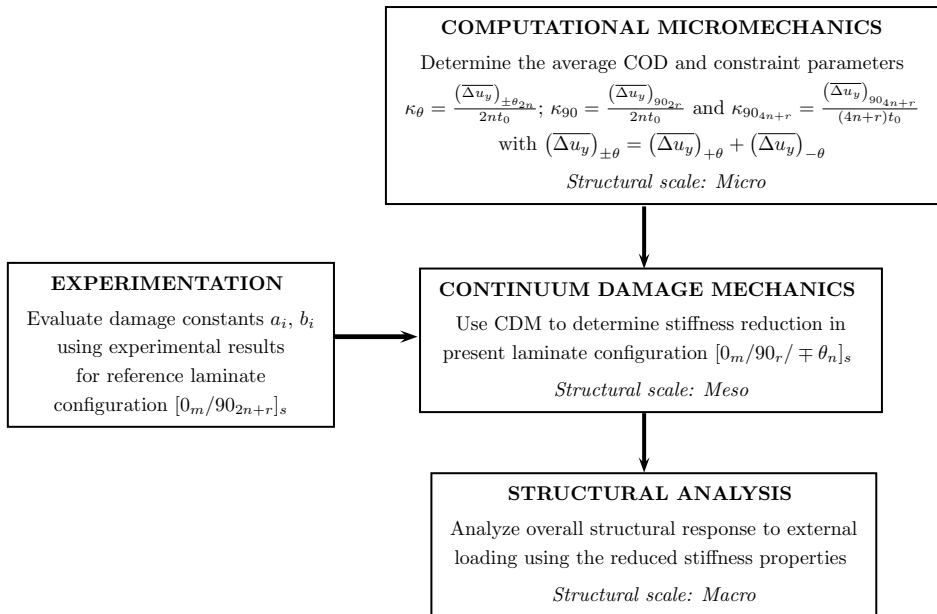


Figure 2: Multi-scale synergistic damage mechanics (SDM) methodology for analyzing damage behavior in a general symmetric laminate $[0_m/90_r/\mp\theta_n]_s$ with matrix cracks in $+\theta$, $-\theta$, and 90° layers

The flowchart in Fig. 2 depicts the overall multi-scale SDM procedure to conduct structural analysis of damaged composite structures for the particular case of $[0_m/90_r/\mp\theta_n]_s$ laminates with ply cracks in $+\theta$, $-\theta$, and 90° layers. As mentioned earlier, this approach combines micromechanics with CDM for a complete evaluation of the structural response. Micromechanics involves FE analysis to determine CODs in cracked plies within an RVE (or unit cell, if applicable), from

which the constraint effect is evaluated. This constraint effect is then carried over in the CDM formulation through the constraint parameters. In a separate step, the damage constants a_i and b_i are determined from the stiffness data for a reference laminate using Eqs. (18)-(19). With the values of the damage constants and constraint parameters known, the stiffness-damage relations described by Eq. (13) and Eq. (20) are utilized to evaluate the variation of elastic moduli with respect to crack density. In order to evaluate the constraint parameters involved in the SDM model described above, we utilized computational micromechanics via three dimensional finite element analysis (FEM). Fig. 3 and Fig. 4 show the FE models for the cases of ply cracking in two orientations, and three orientations, respectively. Further details of FE models for multiple off-axis cracks in multidirectional laminates has been described in earlier reports: Singh and Talreja (2008, 2009); Li, Singh and Talreja (2009); Singh and Talreja (2010). In particular, the definition of the RVE for a laminate with ply cracks in multiple orientations and its implication on the development of corresponding FE model has been covered in Li, Singh and Talreja (2009). As expected from above discussion, the major parameter that is evaluated using these FE analyses is the average COD for ply cracks in each damage mode.

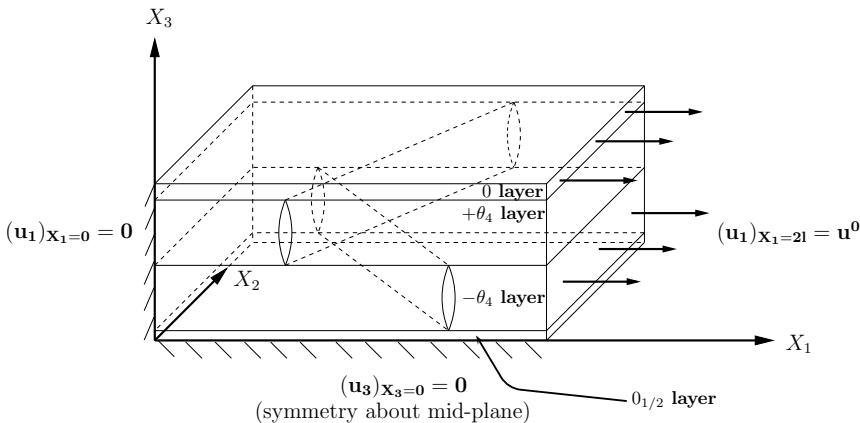


Figure 3: A representative unit cell for 3D FE analysis of $[0/\pm\theta_4/0_{1/2}]_s$ laminates. Ply cracks are present in off-axis $\pm\theta$ layers.

3 Results and discussion

In this section we describe the predictions of elastic moduli changes with crack density using the higher order SDM model described above for a broad range of multidirectional composite layup configurations. A comparison with previously

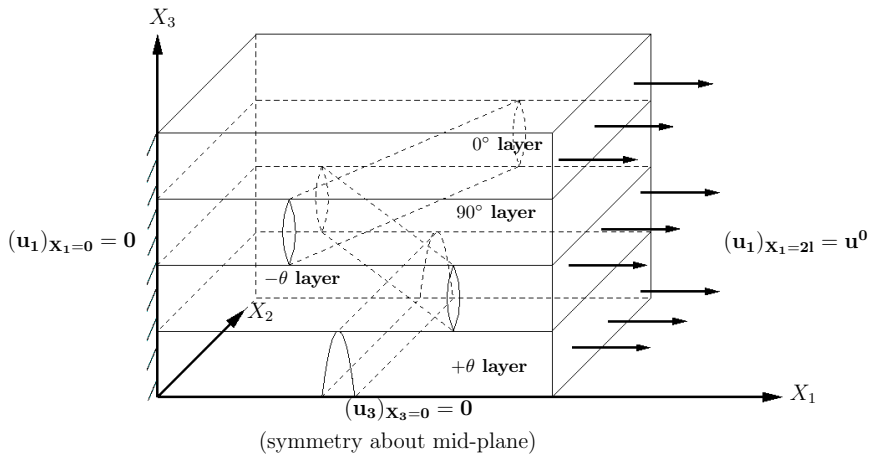


Figure 4: A representative unit cell for 3D FE analysis of $[0/90/\mp\theta]_s$ laminate. Ply cracks are present in three orientations: 90° , $+\theta$ and $-\theta$.

developed linear damage models as well as independent experimental data is also provided. In the following subsections, we cover three different cases for ply cracking involving: a single damage mode; two damage modes; and three damage modes. The experimental data chosen here is specifically taken from a variety of researchers so as to validate the model presented in the current study over a wider range of laminate geometry and manufacturing processes.

3.1 Stiffness changes in $[\pm\theta_m/90_n]_s$ laminates

In order to showcase the applicability and usefulness of the higher order damage model over linear models, let us first consider the laminate configuration where cracks are present in the transverse (90°) plies only. The reference laminate chosen for this layup is $[0_2/90_4]_s$, a crossply laminate of similar class of laminates. The damage constants a_i and b_i for the chosen reference laminate are determined from this data using Eqs. (18)-(19). The changes in the overall stiffness properties of the laminates brought about by ply cracking damage in 90° plies are then predicted using the stiffness-damage relations, Eq. (13), and the relative constraint parameter, Eq. (23).

The laminate material is glass epoxy with the following ply properties: ply thickness, $t_0=0.144$ mm, longitudinal Young's modulus, $E_1 = 44.73$ GPa, transverse modulus, $E_2 = 12.76$ GPa, in-plane shear modulus, $G_{12} = 5.8$ GPa and Poisson's ratio, $\nu_{12} = 0.297$. The unidirectional ply is assumed to be transversely isotropic in the cross-sectional plane with a Poisson's ratio $\nu_{23} = 0.42$. The relative constraint

parameter in Eq. (23) for varying θ was calculated to be equal to $\kappa_{rel}(\theta = 15^\circ) = 1.03$, $\kappa_{rel}(\theta = 30^\circ) = 1.09$, $\kappa_{rel}(\theta = 40^\circ) = 1.15$. When compared to investigations performed in Varna, Joffe and Talreja (2001), the parameters obtained here are slightly different; mainly because the cited study performed a 2D FE analysis for their calculations. Furthermore, there might be differences in the model sizes in the longitudinal direction, i.e. the crack spacing at which average CODs are computed. Nonetheless, the differences in the overall stiffness changes using CODs calculated in the the cited study and in the present work and using a linear SDM model are relatively minor. Therefore, they should not affect our observations.

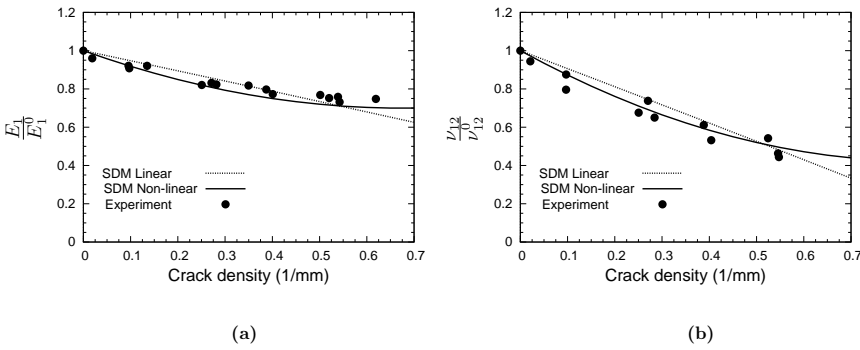


Figure 5: Stiffness reductions for $[0_2/90_4]_s$ laminate compared with experimental results reported by Varna, Joffe and Talreja (2001). The moduli are normalized with respect to their magnitude for pristine laminates. These results form the basis for computation of SDM constants. The linear damage model is also from Varna, Joffe and Talreja (2001).

Fig. 5 shows the variation of the longitudinal Young's modulus and the Poisson's ratio with respect to crack density for the reference laminate. The moduli values shown in the figure are normalized with the corresponding virgin state values. The linear continuum damage model, developed by Varna, Joffe and Talreja (2001), is also shown for the sake of comparison. These results form the basis for calculation of damage constants a_i , b_i in the SDM model. While computing the damage constants, experimental data at crack densities $\rho_1 = 0.5$, and $\rho_2 = 0.65$ were utilized.

Once the damage constants are known for this class of laminate layup, SDM stiffness-damage relations, Eqs. (13), (14) can be used to predict stiffness changes in laminates with other θ values. For the case of $\theta = 15^\circ, 30^\circ$ and 40° degrees, the non-linear SDM predictions, along with linear damage model as well as the experimental data, are shown in Fig. 6 - Fig. 8. It should be noted here that the cracks are still assumed only in the 90° plies. In general, both linear and nonlinear damage model

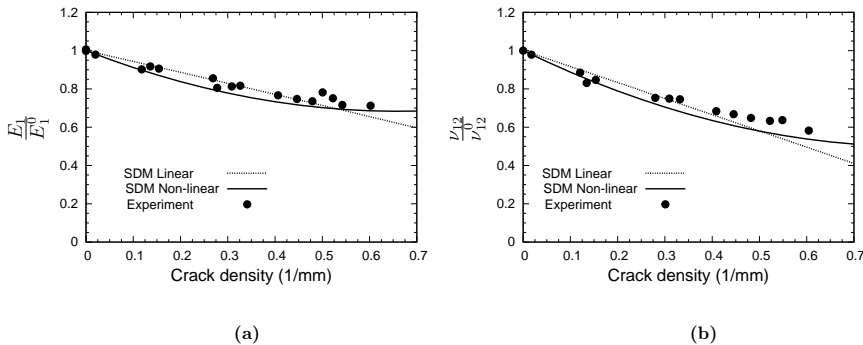


Figure 6: Nonlinear SDM model predictions for stiffness reduction in $[\pm 15/90_4]_s$ laminate compared with experimental results and the linear damage model, both from Varna, Joffe and Talreja (2001).

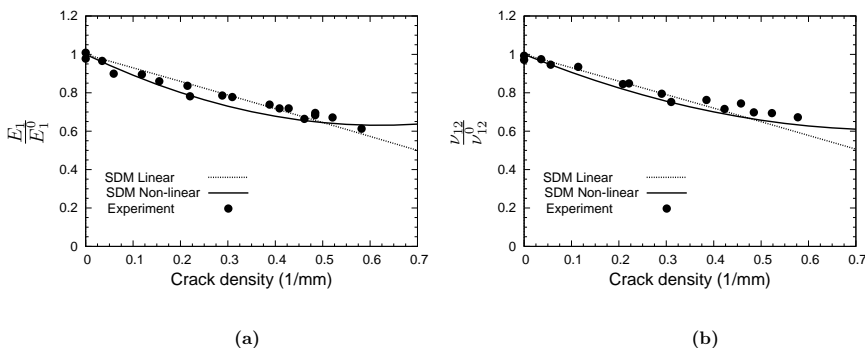


Figure 7: Nonlinear SDM model predictions for stiffness reduction in $[\pm 30/90_4]_s$ laminate compared with experimental data and the linear damage model, both from Varna, Joffe and Talreja (2001).

predictions for axial modulus and Poisson's ratio show reasonable agreement with the test data. They are also good at predicting the overall trends in stiffness degradation while going from the case of crossply laminates, $\theta = 0^\circ$, to the case where $\theta = 40^\circ$. However, on closer inspection, it can be observed that the linear SDM model usually under-predicts the stiffness changes in the beginning of damage evolution, while it over-predicts the degradation in the damage effects at large crack densities. This effect is particularly obvious for the case of $\theta = 30^\circ$ and 40° , see Figs. 7, 8. The nonlinear SDM predictions, on the other hand, seem to follow experimental trends more closely. In the case of linear damage models, there are four damage constants (a_i) which are determined using the test data for stiffness

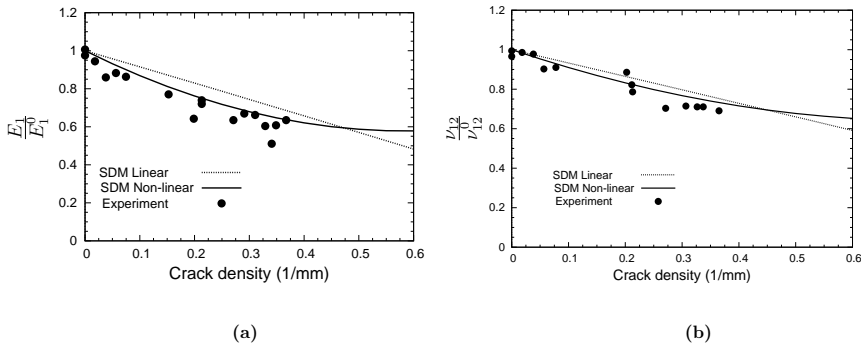


Figure 8: Nonlinear SDM model predictions for stiffness reduction in $[\pm 40/90_4]_s$ laminate compared with test data and the linear damage model, both from Varna, Joffe and Talreja (2001).

changes at a single crack density, ρ . It is observed that the predictions from the linear model are sensitive to the choice of crack density at which the experimental data is used for determination of damage constants. This choice seems to be somewhat heuristic in nature, and affects the accuracy of model predictions. The higher order model seems to be less sensitive to this limitation.

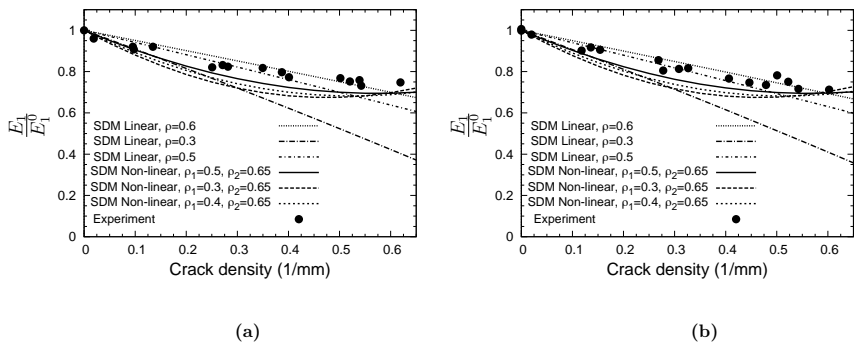


Figure 9: Sensitivity of linear and non-linear damage models on the choice of crack densities at which stiffness degradation data is used to obtain damage constants. As shown here are the variation of longitudinal Young's moduli for (a) $[0_2/90_4]_s$ laminate, and (b) $[\pm 15/90_4]_s$ laminate. The moduli are normalized with respect to their magnitude for pristine laminates. The experimental data is from Varna, Joffe and Talreja (2001).

To better explain this behavior, the predictions for longitudinal Young's moduli for

$[0_2/90_4]_s$ and $[\pm 15/90_4]_s$ laminates are shown in Fig. 9 for multiple choices of crack densities that were used in the determination of damage constants. For the linear model, it can be clearly seen that if the stiffness degradation data from experiments is chosen earlier in the damage development ($\rho < 0.4$), its predictions are extremely inaccurate at high crack densities. The non-linear model, however, shows less sensitivity while also maintaining conservative predictions of the elastic moduli for the damaged laminate. It is also noted that if ρ_2 is not chosen properly, in some cases the nonlinear predictions start showing negative stiffness degradation, apparent from Fig. 9(b) above $\rho = 0.5$. Since $\rho \rightarrow \infty$ represents the limiting stiffness contribution from uncracked plies that can be easily computed using the ply-discount method, setting $\rho_2 = \infty$ will resolve this issue. This will also eliminate the need to obtain experimental data for more than one crack density.

3.2 Stiffness changes in $[0/\pm\theta_4/0_{1/2}]_s$ laminates

Next we take up the case of multidirectional laminates with ply cracking damage in two damage modes. The corresponding experimental data are available from Varna, Joffe, Akshantala and Talreja (1999). Each ply is 0.125 mm thick, and the ply material is glass-epoxy (HyE 9082Af, Fiberite) with in-plane properties $E_1=44.7$ GPa, $E_2=12.7$ GPa, $G_{12}=5.8$ GPa and $\nu_{12}=0.297$. In the class of laminates chosen here, ply cracking is assumed to initiate in both $\pm\theta$ plies simultaneously, consistent with experimental observations and earlier analyses. Furthermore, it is assumed that the cracks grow at identical rates and cause identical changes in laminate's stiffness properties. Hence, the constraint effects in two damage modes, $+\theta$ and $-\theta$, can be combined to yield one effective constraint parameter. The applicability of this assumption is detailed in our previous report [Singh and Talreja (2008)], wherein the linear SDM model was developed. The laminate sequence with $\theta = 90^\circ$, i.e. $[0/90_8/0_{1/2}]_s$ is chosen as the reference laminate for evaluation of the damage constants. The variation of normalized longitudinal Young's modulus and the Poisson's ratio with respect to the crack density for the reference laminate are shown in Fig. 10. This figure forms the basis for calculations of damage constants for the present class of laminates undergoing damage in $\pm\theta$ -plies. While computing the damage constants, experimental data at crack densities $\rho_1 = 0.5$, and $\rho_2 = 1.0$ were utilized.

Once the damage constants are determined for the present class of multidirectional laminates, Eqs. (13)-(14) are used to predict effects of damage on overall stiffness properties for laminates with different θ values. The relative constraint parameter is evaluated for the corresponding laminate sequence using Eq. (24). For details on how constraint effects from the supporting plies play a role in modifying the average COD, the reader is referred to Singh and Talreja (2008). The investigation

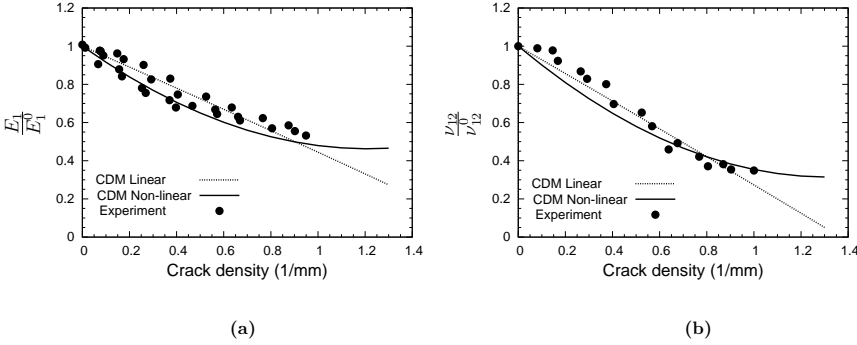


Figure 10: Stiffness reductions for $[0/90_8/0_{1/2}]_s$ laminate compared with experimental results [Varna, Joffe, Akshantala and Talreja (1999)]. These results form the basis for computation of SDM damage constants. The linear damage model shown here is developed in Singh and Talreja (2008).

carried out in the above reference performed an in-depth parametric study of COD variation due to changes in the laminate configuration, e.g. the thickness of the cracked plies, the number (or thickness) of supporting plies, relative stiffness of cracking and supporting plies, and the cracked ply orientation. As a summary, it was understood that change in the number or total thickness of cracking ply was the most influential factor because an increase in the number of cracked plies (for a fixed number of supporting plies) implies a corresponding increase in the ply crack size. Larger crack size results into larger average COD values and consequently a steeper stiffness degradation. An increase in the thickness, or the number or higher relative stiffness of constraining plies, on the other hand, caused degradation in stiffness properties to a lesser degree. Utilizing these parametric studies, a master equation was developed to combine the effects of these geometric and material variables. For the case of non-interactive damage modes, the average COD was determined to be equal to

$$\overline{(\Delta u_y)}_{\pm\theta_n} = U \cdot f_1(\theta) \cdot f_2(r) \cdot f_3(m) \cdot f_4(n) \tag{28}$$

where, U is the average COD for the reference laminate $[0/90_8/0_{1/2}]_s$, and f_1 to f_4 are parametric functions fitted to the FE results for average COD. Please see Singh and Talreja (2008) for further details.

Using this relation for average COD and the nonlinear SDM stiffness-damage relations, stiffness changes are obtained for $[0/\pm 70_4/0_{1/2}]_s$ laminate (see Fig. 11). The nonlinear SDM predictions for the axial moduli show good agreement with the experimental data, whereas the linear model does not follow the experimental

trends at high laminate. Also, it is important to compare the degree of nonlinearity in stiffness changes on going from $\theta = 90^\circ$ to $\theta = 70^\circ$. As θ decreases, the test data suggests an increasing nonlinearity in the stiffness degradation. The linear damage model misses this pattern, while it is captured well by the higher order SDM model. For the case of Poisson's ratio, experimental data depicts severe degradation early on during the damage evolution, and both models show reasonable correspondence. However, here also, the higher order approach seems to fare better than the linear model.

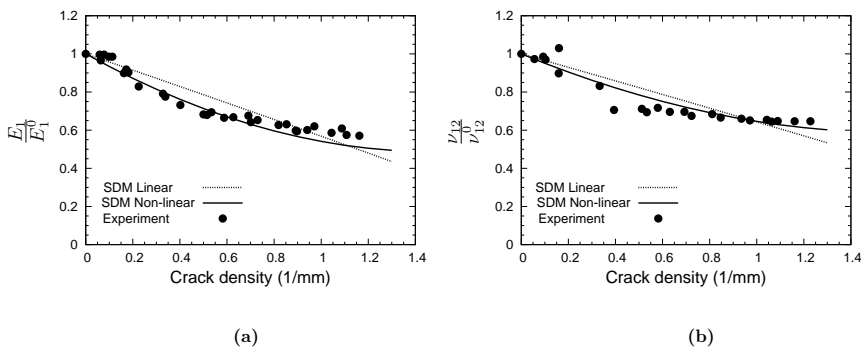


Figure 11: Nonlinear SDM model predictions for stiffness degradation in $[0/\pm 70_4/0_{1/2}]_s$ laminate in comparison with experimental data [Varna, Joffe, Akshantala and Talreja (1999)]. The linear damage model shown here is described in Singh and Talreja (2008).

3.3 Stiffness changes in quasi-isotropic ($[0/90/\mp 45]_s$) laminates

The experimental data for stiffness changes brought about by multi-mode ply cracking in multidirectional laminates are quite limited. One important laminate layup investigated so far is the quasi-isotropic laminate that involves a mix of 90° , $+45^\circ$ and -45° layers in a manner to obtain isotropic stiffness properties in its pristine condition. Tong, Guild, Ogin and Smith (1997) performed extensive measurements on the initiation and progression of ply cracking damage in $[0/90/\mp 45]_s$ laminates; and its effect on the overall stiffness behavior.

The reference laminate chosen for this case was again the crossply laminate ($[0/90_3]_s$). For evaluating the damage constants, FE data for stiffness property changes as a function of crack density were utilized. The methodology for calculation of stiffness changes due to this damage scenario using FE approach is described in Singh and Talreja (2009). FE analysis was also performed to calculate the average COD

values for cracks in all cracked ply orientations and corresponding constraint parameters. The individual ply thickness for this laminate is 0.5 mm with in-plane properties: $E_1=46$ GPa, $E_2=13$ GPa, $G_{12}=5$ GPa and $\nu_{12}=0.3$. The corresponding constraint parameters are calculated as: $\kappa_{90_{4n+2r}} = 6.1e-3$, $\kappa_{\theta}|_{\theta=90} \approx \kappa_{90} = 5.4e-3$, $\kappa_{\theta+} = 3.97e-3$, $\kappa_{\theta-} = 3.35e-3$, $\kappa_{\theta} = \frac{1}{2}(\kappa_{\theta+} + \kappa_{\theta-}) = 3.66e-3$.

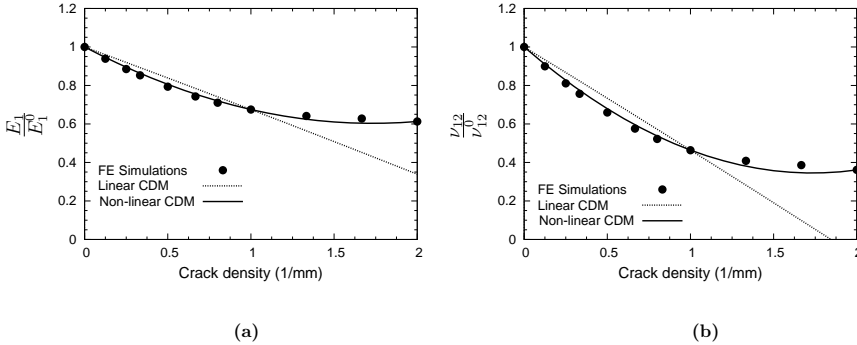


Figure 12: Stiffness reductions for $[0/90_3]_s$ laminate compared with 3D FE simulation predictions for stiffness changes. The linear damage model is developed in Singh and Talreja (2009). This figure forms the basis for computation of damage constants for this class of laminate layup.

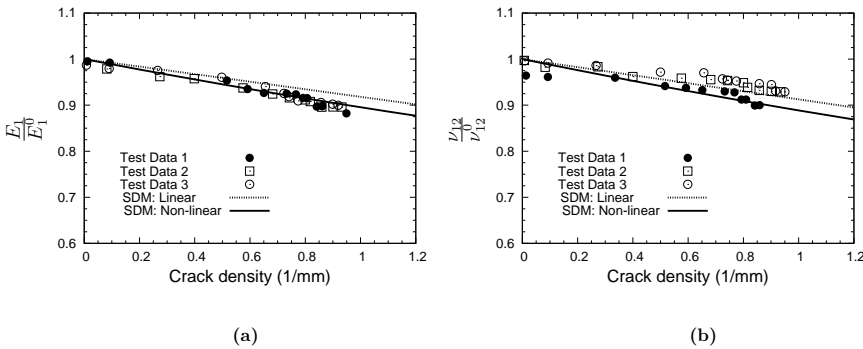


Figure 13: Nonlinear SDM model predictions for stiffness changes in quasi-isotropic $([0/90/\pm 45]_s)$ laminate compared with experimental data [Tong, Guild, Ogin and Smith (1997)]. The linear damage model is from Singh and Talreja (2009).

Fig. 12 shows the variation of normalized longitudinal Young’s modulus and the

Poisson's ratio with respect to the crack density for the reference laminate including the FE simulation results, linear damage model from Singh and Talreja (2009) and the current nonlinear model. As in earlier cases, this figure forms the basis for calculation of constants a_i and b_i for the present class of multidirectional laminates. Once the damage constants as well as constraint parameters for different θ values are determined, stiffness changes are calculated using Eq. (13) for quasi-isotropic laminates. Fig. 13 shows the stiffness predictions for the case of $[0/90/\mp 45]_s$ layup with ply cracks in all three off-axis orientations. The figure contains experimental data reported by Tong, Guild, Ogin and Smith (1997), predictions using the linear damage model developed in Singh and Talreja (2009) and predictions from the current nonlinear SDM model. From the plot of axial modulus, it is clear that the linear model tends to under-predict degradation over the whole range of crack densities. However, the nonlinear SDM model captures predictions for both axial modulus and Poisson's ratio to a good level of accuracy, especially considering a wide fluctuation in the test data for Poisson's ratio. Similar to the case of angle-ply laminates, the predictions for current laminate layup from linear SDM model are sensitive to the point where the experimental data is used for determination of damage constants. However, the higher order model seems to be less sensitive to this source of inaccuracy. In a truly multi-mode scenario, the cracks from different damage modes can interact. This interaction can be easily integrated into the proposed model by using COD's for the interactive FE unit cell, as accomplished in Singh and Talreja (2009) for linear SDM models. Overall, these results suggest the usefulness of nonlinear SDM approach over linear models in predicting stiffness reductions.

An accurate damage model is essential for an accurate prediction of the integrity and durability of the composite structures. If the damage model developed here can be integrated with the advanced techniques of structural health monitoring (SHM) and non-destructive evaluation (NDE), a real-time health monitoring tool can be developed. Such a tool will lead to significant positive impact on the safety and longevity of the composite structures. The NDE techniques can help us determine the crack density in the component, then the proposed theory can be used to predict the resulting stiffness and an assessment can be made if the part is still serviceable. These developments will eventually lead to more accurate and cost-effective design of composite structures.

4 Conclusion

The synergistic damage mechanics approach combines the strengths of continuum damage mechanics approach with computational micromechanics to predict changes in the stiffness properties of composite laminates due to ply cracking.

Recently, the SDM methodology was extended to multiple multi-mode damage scenarios. In particular, stiffness changes in damaged composite laminates with ply cracking in two and three orientations has been explored in Singh and Talreja (2008, 2009). However, a key limitation of both CDM and SDM models has been the linearized stiffness-damage relationships. Consequently, the current predictions of these approaches show linear stiffness property reductions, in contradiction with the available experimental data which suggest nonlinear stiffness changes, particularly at larger crack density levels. The test data over a wide range of laminate systems shows a larger decrease in the beginning of damage development, and a lesser decrease when damage has developed to an appreciable extent, leading to a limiting minimum stiffness dictated by the contributions from uncracked plies. This paper was targeted to alleviate this limitation by extending the SDM approach to second order damage coefficients. The free energy expression necessary to derive stiffness relations is expanded to include non-linear damage terms and corresponding stiffness-damage relations are derived for angle ply, off-axis and quasi-isotropic laminate configurations.

Based on the comparison of both linear and nonlinear SDM models with experimental data, it can be concluded that the higher order SDM model works significantly better than the linear model for crack density higher than 0.8 cr/mm. It also shows a good level of accuracy over the whole range of crack densities. Additionally, the nonlinear damage model shows consistency in predictions over a wide range of laminate layups, with widely different damage scenarios. For some laminates, the linear model under-predicts the stiffness changes, especially in the initial stages of damage development. The nonlinear model does not suffer from this limitation and shows good agreement with the test data. In cases where there is a significant interaction between adjacent cracks (at high crack density), CODs should be evaluated using an interactive FE unit cell with appropriate crack spacing. Finally, it was observed that the predictions from the linear model are sensitive to the point where uses for the experimental data in determination of damage constants. However, the higher order model seems to be less sensitive to this.

With earlier reports and the present study focused on the development of SDM approaches, a good level of confidence has been achieved over their applicability to a broad range of laminate configurations and the accuracy of their stiffness predictions. Our next focus will be to implement these models into finite element packages to enable commercial application. Nonetheless, some issues remain unresolved. For instance, the effects of multi-axial loading have not been addressed so far. Furthermore, the development and application of such approaches under cyclic loading remains elusive. Modeling effort so far has targeted design approaches based on sub-critical damage only. However, often the damage scenario may in-

volve both sub-critical and critical damage mechanisms simultaneously. Both sub-critical and critical damage mechanisms contribute to the non-linear stress strain response of the material. In such cases, the present model needs to be extended to include these damage mechanisms in an appropriate fashion. FE implementation also needs careful attention as the material behavior would be mesh-dependent subsequent to a significant loss in elastic properties due to damage. If we achieve these goals, only then an accurate analysis of damage development and progressive failure in industrially relevant composite structures is feasible.

References

- Allen, D. H.; Harris, C. E.; Groves, S. E.** (1987): A thermomechanical constitutive theory for elastic composites with distributed damage.2. application to matrix cracking in laminated composites. *Int J Solids Struct*, vol. 23, no. 9, pp. 1319–1338.
- Gudmundson, P.; Ostlund, S.** (1992): Prediction of thermoelastic properties of composite laminates with matrix cracks. *Compos Sci Tech*, vol. 44, no. 2, pp. 95–105.
- Hashin, Z.** (1985): Analysis of cracked laminates: a variational approach. *Mech Mater*, vol. 4, no. 2, pp. 121–136.
- Joffe, R.; Krasnikovs, A.; Varna, J.** (2001): COD-based simulation of transverse cracking and stiffness reduction in [S/90n]_s laminates. *Compos Sci Tech*, vol. 61, no. 5, pp. 637–656.
- Li, S.; Singh, C. V.; Talreja, R.** (2009): A representative volume element based on translational symmetries for FE analysis of cracked laminates with two arrays of cracks. *Int J Solids Struct*, vol. 46, pp. 1793–1804.
- Lundmark, P.; Varna, J.** (2005): Constitutive relationships for laminates with ply cracks in in-plane loading. *Int J Dam Mech*, vol. 14, no. 3, pp. 235–259.
- Mccartney, L. N.** (1992): Theory of stress transfer in a 0-degrees-90-degrees-0-degrees cross-ply laminate containing a parallel array of transverse cracks. *J Mech Phys Solids*, vol. 40, no. 1, pp. 27–68.
- Singh, C. V.; Talreja, R.** (2008): Analysis of multiple off-axis ply cracks in composite laminates. *Int J Solids Struct*, vol. 45, no. 16, pp. 4574–4589.
- Singh, C. V.; Talreja, R.** (2009): A synergistic damage mechanics approach for composite laminates with matrix cracks in multiple orientations. *Mech Mater*, vol. 41, no. 8, pp. 954–968.
- Singh, C. V.; Talreja, R.** (2010): Evolution of ply cracks in multidirectional composite laminates. *Int J Solids Struct*, vol. 47, pp. 1338–1349.

Singh, C. V.; Talreja, R. (2013): A synergistic damage mechanics approach to mechanical response of composite laminates with ply cracks. *J Compos Mater*, vol. DOI: 10.1177/0021998312466121, no. 8.

Talreja, R. (1985): A continuum mechanics characterization of damage in composite materials. *Proc Royal Soc London A*, vol. 399, no. 1817, pp. 195–216.

Talreja, R. (1990): Internal variable damage mechanics of composite materials. In Boehler, J. P.(Ed): *Yielding, Damage, and Failure of Anisotropic Solids*, pp. 509–533. Mechanical Engineering Publications, London.

Talreja, R. (1994): Damage characterization by internal variables. In Talreja, R.(Ed): *Damage Mechanics of Composite Materials*, pp. 53–78. Elsevier, Amsterdam.

Talreja, R. (1996): A synergistic damage mechanics approach to durability of composite material systems. In Cardon, A.; Fukuda, H.; Reifsnider, K.(Eds): *Progress in durability analysis of composite systems*, pp. 117–129. A.A. Balkema, Rotterdam.

Talreja, R.; Singh, C. V. (2012): *Damage and Failure of Composite Materials*. Cambridge University Press, London. ISBN: 9780521819428.

Tong, J.; Guild, F. J.; Ogin, S. L.; Smith, P. A. (1997): On matrix crack growth in quasi-isotropic laminates - i. experimental investigation. *Compos Sci Tech*, vol. 57, no. 11, pp. 1527–1535.

Varna, J.; Akshantala, N. V.; Talreja, R. (1999): Crack opening displacement and the associated response of laminates with varying constraints. *Int J Dam Mech*, vol. 8, no. 2, pp. 174–193.

Varna, J.; Joffe, R.; Akshantala, N. V.; Talreja, R. (1999): Damage in composite laminates with off-axis plies. *Compos Sci Tech*, vol. 59, no. 14, pp. 2139–2147.

Varna, J.; Joffe, R.; Talreja, R. (2001): A synergistic damage-mechanics analysis of transverse cracking in $[\pm\theta/90]_s$ laminates. *Compos Sci Tech*, vol. 61, no. 5, pp. 657–665.

